ELSEVIER

Chemical Engineering Journal 89 (2002) 203–211

Chemical Engineering Journal

www.elsevier.com/locate/cej

Analysis of gas–liquid mass transfer in an airlift contactor with perforated plates

Sontaya Krichnavaruk, Prasert Pavasant*

Faculty of Engineering, Department of Chemical Engineering, Chulalongkorn University, Bangkok 10330, Thailand

Abstract

This work investigated roles of an perforated plate on the gas–liquid mass transfer in an airlift contactor (ALC), and it was found that the effect of the perforated plate was twofold. Firstly, it helped in breaking up large bubbles that passed through the plate. It was observed that inserting a perforated plate could increase the interfacial area between gas and liquid to more than twice its original value. Secondly, the presence of a perforated plate seemed to lower down the mass transfer coefficient between the two phases. The analysis showed that the effect of the increase in the interfacial area between gas and liquid exceeded that of the reduction in the mass transfer coefficient. Hence, the overall rate of gas–liquid mass transfer in the employed ALC was found to be enhanced when perforated plates were inserted into the system. The effect of the configuration of perforated plate, i.e. hole size, number of hole, and the number of perforated plate, was also investigated.

Keywords: Airlift contactor; Perforated plate; Gas–liquid mass transfer

1. Introduction

Although airlift contactors (ALCs) have gained enormous attention as a new alternative reactor particularly for biochemical processes, they suffer a serious drawback due to their relatively low rate of gas–liquid mass transfer. Investigators have concentrated on the enhancement of this process and several new designs of ALCs have been proposed [1–8]. Among these investigations, inserting baffles or perforated plates in the riser of the ALC was reported to be one of the successful methods for improving the system mass transfer performance [6,9,10]. Perforated plates in the ALC were found to facilitate the breakage mechanism of bubbles which resulted in a higher mass transfer area between gas and liquid.

This work focuses on the in-dept investigation of the role of the perforated plate on the gas–liquid mass transfer inside the ALC. A photographical technique is employed to examine bubble forming/breaking phenomena in the system with perforated plates inserted into the riser. The influence of the perforated plate on the specific mass transfer area and on the specific rate of gas–liquid mass transfer will be quantified.

* Corresponding author. Tel.: +66-2218-6870; fax: +66-2218-6877.
E-mail address: prasert.p@chula.ac.th (P. Pavasant).

2. Experimental

The ALC employed in this work is diagrammatically shown in Fig. 1. The contactor was made of clear acrylic plastic to enable visual observation of system behavior. The column was 240 cm high with a diameter of 11 cm (including wall thickness of 6 mm), and the 207 cm high draft tube with an inside diameter of 7.4 cm (3 mm wall thickness) was fitted centrally inside the outer column with a 5 cm vertical space above the base of the outer column.

The overall gas holdup was estimated using the volume expansion method where the overall gas holdup, ε_{Go}, was calculated from the dispersion height, H_D, and the unaerated liquid height, H_L following the expression:

$$\varepsilon_{Go} = \frac{H_D - H_L}{H_D} \tag{1}$$

The manometer connected to the side of the main column was employed for the pressure drop measurement which was then used to calculate gas holdups both in downcomer, ε_{Gd}, and in gas separator, ε_{Gs}. The riser gas holdup, ε_{Gr}, was subsequently estimated using the following overall gas holdup expression:

$$\varepsilon_{Go} = \frac{H_{DT}A_r\varepsilon_{Gr} + H_{DT}A_d\varepsilon_{Gd}}{H_D(A_r + A_d)} + \frac{(H_D - H_{DT})(A_d + A_r)\varepsilon_{Gs}}{H_D(A_r + A_d)} \tag{2}$$

1385-8947/02/$ – see front matter
PII: S1385-8947(02)00010-4

Nomenclature

a	specific gas–liquid interfacial area (cm^{-1})
a_c	specific gas–liquid interfacial area in a conventional ALC (cm^{-1})
a_i	specific gas–liquid interfacial area in section i (cm^{-1})
a_T	overall/average specific gas–liquid interfacial area in the ALC with perforated plate(s) (cm^{-1})
A_B	total gas–liquid interfacial area (cm^2)
A_d/A_r	ratio between downcomer cross-sectional area to riser cross-sectional area (–)
d_B	equivalent bubble diameter (cm)
d_{Bs}	Sauter mean diameter of bubble (cm)
k_L	coefficient ($cm\,s^{-1}$)
k_La	overall volumetric mass transfer coefficient (s^{-1})
k_La_c	overall volumetric mass transfer coefficient in conventional concentric ALC (s^{-1})
k_La_T	overall volumetric mass transfer coefficient in ALC with a perforated plate (s^{-1})
U_{sg}	superficial gas velocity ($cm\,s^{-1}$)
V_i	fluid volume in section i (cm^3)

Greek letter

ε	gas holdup (–)

where H_{DT}, A_r, and A_d are the height of draft tube, the cross-sectional areas of riser and downcomer, respectively.

The measuring ports were also used for the injection of color tracer in the measurement of liquid velocities. The downcomer liquid velocity, V_{Ld}, was calculated from the time the tracer required to travel between any two points in the column, t_d:

$$V_{Ld} = \frac{L_d}{t_d} \tag{3}$$

where L_d is the distance between two observation points. Note that in this experiment, the measurement was performed in the downcomer and the riser liquid velocity was calculated based on the circulating liquid volumetric flowrate.

In the operation of the ALC, the column was first filled with tab water until the unaerated water level was 5 cm above the draft tube height. Air was then sparged centrally through a porous sparger at the base of the contactor, and the aerated rate was controlled by a calibrated rotameter with minimum and maximum superficial velocities (U_{sg}) of 1.8 and 8.4 $cm\,s^{-1}$, respectively. Note that the superficial gas velocity was calculated based on the cross-sectional area of riser. The DO meter (Jenway model 9300) was located in the column to measure changes in the dissolved oxygen concentration in the dispersion. The rate of gas–liquid mass transfer and the overall volumetric mass transfer coefficient, k_La, were then calculated from the rate of oxygen being transferred from gas to liquid phases:

$$\frac{dC}{dt} = k_La(C^* - C) \tag{4}$$

where C is the bulk concentration of dissolved oxygen, and C^* the saturated concentration of dissolved oxygen.

The experiment was also carried out in a bubble column (BC) and a conventional ALC with the same column diameter as the ALC with perforated plates. The size and number of holes in the perforated plate were varied to investigate the effect of plate configuration on the rate of gas–liquid mass transfer. The number of perforated plates was also variable from 1 to 3. Detail of the perforated plates is given in Fig. 2.

The bubble size was measured using a digital video-recorder (SONY, DCR-TRV 20E). For ellipsoidal bubbles, the major and minor axes of the bubble images were measured. The equivalent size of the bubble (d_B), which is the diameter of the sphere whose volume is equal to that of the bubble, can then be calculated using the following relationship:

$$d_B = (x^2y)^{1/3} \tag{5}$$

where x and y are major and minor axis lengths of the ellipsoid. These axes are illustrated in the example of digital photograph in Fig. 3. The Sauter mean diameter, d_{Bs}, was subsequently calculated from d_B using the following equation [11]:

$$d_{Bs} = \frac{\sum_{i=1}^{n} d_B^3}{\sum_{i=1}^{n} d_B^2} \tag{6}$$

where n is a number of sampling bubbles which, in this experiment, was around 200–300. The specific interfacial area between gas bubble and liquid, a, was then calculated from:

$$a = \frac{6\varepsilon}{d_{Bs}(1-\varepsilon)} \tag{7}$$

where ε is the local gas holdup.

3. Results and discussion

Fig. 4 shows comparisons between performances of the ALC with and without a perforated plate and the BC. It is clear that inserting the perforated plate reduced the circulating liquid velocity and consequently increased riser gas holdup significantly. The overall rate of gas–liquid mass transfer (which was indicated in terms of overall volumetric mass transfer coefficient, k_La) was also found to be augmented by the perforated plate. The following discussion attempts to investigate effects of this perforated plate on the rate of mass transfer (k_L) and the specific interfacial area (a) between gas bubble and liquid individually using the information of the measurement of bubble size and gas holdup in the system.

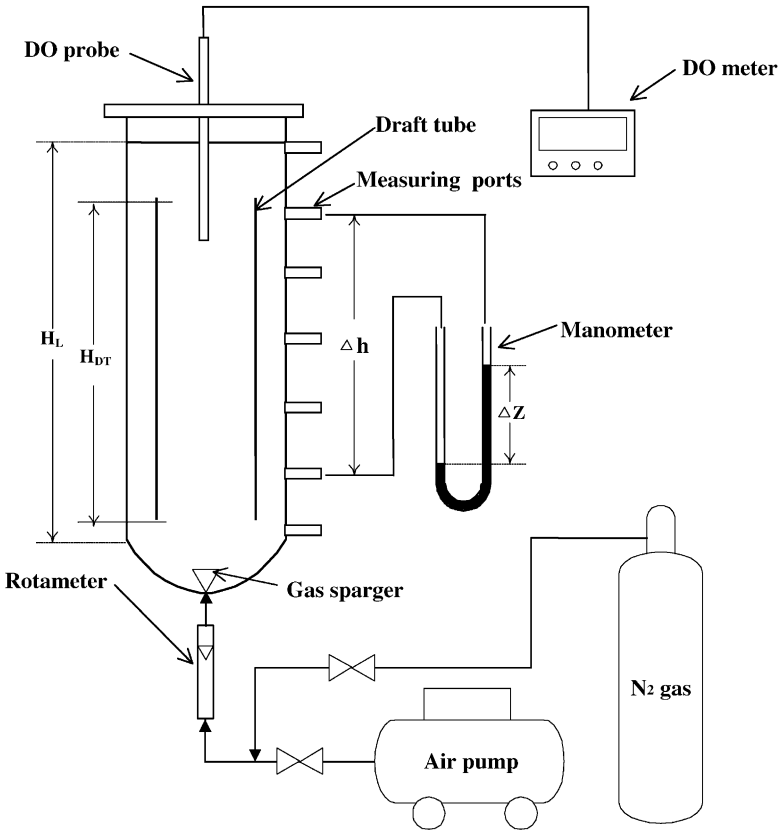

Fig. 1. Setup of experimental apparatus.

Fig. 3 shows an example of the digital photograph taken from the experiment which clearly illustrated the role of perforated plate in breaking large bubbles into smaller ones. However, bubbles were observed to coalesce again once they left the perforated plate, and their size after the coalescence was approximately equal to the size before they reached the plate. There existed a certain upflow distance that bubbles needed to travel in order to coalesce, and in this work, this distance was observed to be around 3–5 cm depending on operating conditions of the ALC and the configuration of the perforated plate. Unfortunately, stand-still pictures could not clearly demonstrate this distance as well as digital VDO images which were not shown in this article. The average sizes of the bubbles at various section in the ALC, e.g. before and after reaching the perforated plate, were measured from the photographs. This information along with data of local gas holdups (both in riser and downcomer) were then employed to estimate the percentage increase in the interfacial area between gas and liquid in the ALC.

Fig. 5 is sketched to describe regions of different bubble sizes in the ALC with one perforated plate inserted at the middle of the riser. These various regions took place due to bubbles forming and breaking phenomena when they passed through the perforated plate. Compressed air was sparged through a porous sparger installed at the center of the base of the reactor where gas bubbles with diameter d_1 were formed and flowed along Region 1 (height H_1) with an uniform diameter. Region 1* (height H_1^*) was the intermediate region where small bubbles from the sparger still coalesced to form "d_1 diameter" bubbles. This meant that gas bubbles left the sparger with diameter d_1^* and then rapidly coalesced into a larger size with diameter of d_1 (similar findings can be found in the report by Otake et al. [12]). However, this intermediate region was visually observed to be insignificant as $H_1^* \ll H_1$. When bubbles with d_1 diameter passed through the perforated plate, located midway through the riser, they were broken into smaller size bubbles with diameter d_2 and flowed along the column within Region 2 (height H_2). After that, these bubbles re-coalesced to form larger bubbles with diameter d_3. In Region 3, located above Region 2 with the height of H_3, an average bubble diameter was most of the time observed to be approximately the same as that in H_1 ($d_3 \cong d_1$ from digitally recorded evidence). Hence, it might be reasonable to conclude that bubble characteristics within Region 3 was the same as those within Region 1. To calculate the percentage increase in the specific interfacial mass transfer area, the following calculation is carried out:

$$A_B = a_T V_T = a_1 V_1 + a_2 V_2 + a_3 V_3 \quad (8)$$

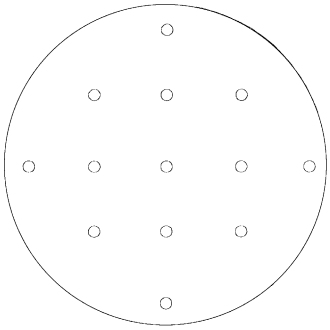

Configuration of plate with 13 perforated holes

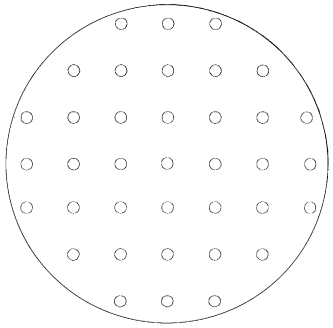

Configuration of plate with 37 perforated holes

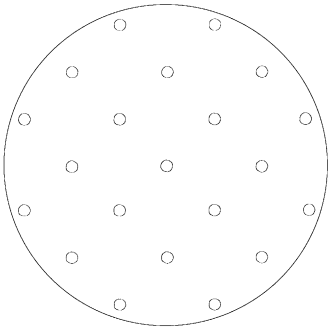

Configuration of plate with 21 perforated holes

Plate*	Hole size diameter (mm)	Number of holes
A-1	3	13
A-2	3	21
A-3	3	37
B-1	4	13
B-2	4	21
B-3	4	37
C-1	5	13
C-2	5	21
C-3	5	37

* Plate diameter = 7.4 cm
The number of plate in each experiment varied from 1 to 3.

Fig. 2. Geometry of perforated plates employed in this work.

The fluid volume in each section can be calculated from the product between cross-sectional area (A) and the dispersion height (H_i), therefore:

$$A_B = a_T A H_T = a_1 A H_1 + a_2 A H_2 + a_3 A H_3 \quad (9)$$

Divide Eq. (3) by $a_1 A$ gives:

$$\frac{a_T}{a_1} H_T = H_1 + \frac{a_2}{a_1} H_2 + \frac{a_3}{a_1} H_3 \quad (10)$$

For gas–liquid contacting devices, the specific interfacial area, a, varies proportionally with the reciprocal of d_{Bs} (Eq. (7)). In addition, gas holdup (ε_{Go}) in the riser of the ALC was found to be approximately constant independent of the height and, hence

$$\frac{a_2}{a_1} = \frac{d_{B1}}{d_{B2}} \quad (11)$$

and since $a_3 = a_1$, substitute Eqs. (7) and (8) into Eq. (4) gives:

$$a_T = \frac{\left(H_1 + \frac{d_{B1}}{d_{B2}} H_2 + H_3\right) \times a_1}{H_T} \quad (12)$$

The difference in specific interfacial area between the ALC and ALC with a perforated plate can then be calculated from:

$$\%a_{diff} = \left(\frac{a_T - a_c}{a_c}\right) \times 100 \quad (13)$$

Provided that the overall volumetric mass transfer coefficients ($k_L a$) in the two ALCs can be calculated from experimental data, the difference between the mass transfer coefficients ($k_{L,diff}$) in both systems can subsequently be calculated from:

$$\%k_{L,diff} = \left(\left(\frac{k_L a_T}{k_L a_c} \times \frac{a_c}{a_T}\right) - 1\right) \times 100 \quad (14)$$

With the above calculation, it was possible to investigate the effect of perforated plate on both specific interfacial area (a), and the mass transfer coefficient (k_L). Table 1 summarizes results from an analysis of mass transfer performance from the ALC with several setups of perforated plates where the plate was configured with various hole sizes and numbers of holes. Also included in this table are the results from the system with various numbers of perforated plates. Overall, it was found that the overall volumetric mass

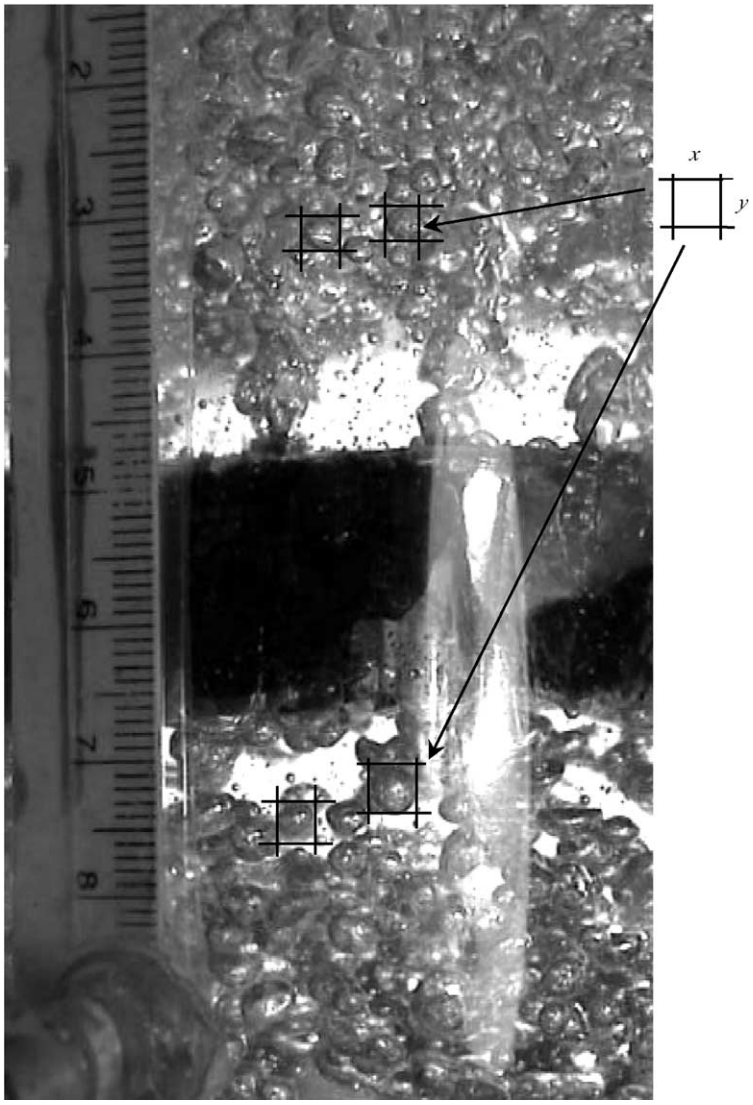

Fig. 3. Example of digital photograph showing bubbles breakage/coalescence at the perforated plate in ALC.

transfer coefficient, $k_L a$, was enhanced by inserting the perforated plate into the ALC. The analysis revealed that this increase in $k_L a$ was due to primary changes in the interfacial mass transfer area (a) as this parameter was highly promoted by the perforated plate, but not the mass transfer coefficient (k_L). For instance, in the case of the ALC with one perforated plate (Plate # B-1: 13 holes with a hole size of 4 mm) at U_{sg} of 1.89 cm s^{-1}, the overall mass transfer coefficient ($k_L a$) was found to be 82.8% more than that in the conventional ALC. Most of this increase was accounted for by the increase in the specific interfacial mass transfer area (a) which was calculated to be about 72%, whilst the mass transfer coefficient (k_L) only contributed as small as 5.9% to the total increase in the overall rate of mass transfer (compared with the performance of the conventional ALC). Interestingly, Table 1 reveals that, in almost all cases investigated in this work, the mass transfer coefficient (k_L) in the ALC with perforated plates was found to be less than that in the ALC. This meant that most of the increase in the overall mass transfer rate was responsible for only by the increase in the interfacial mass transfer area between gas bubble and liquid.

It is apparent from Table 1 that the aerated rate which was expressed in terms of gas superficial velocity, U_{sg}, had two opposite effects on the rate of mass transfer. Firstly, an increase in U_{sg} enhanced the specific interfacial area between gas bubble and liquid which resulted in a better interphase mass transfer. On the other hand, a higher gas throughput reduced the mass transfer coefficient (k_L). However, the effect of the increase in 'a' (specific interfacial area) exceeded the negative influence from the mass transfer coefficient, and within the range of gas velocity employed in this work, the overall volumetric mass transfer coefficient, $k_L a$, was found to increase with U_{sg}.

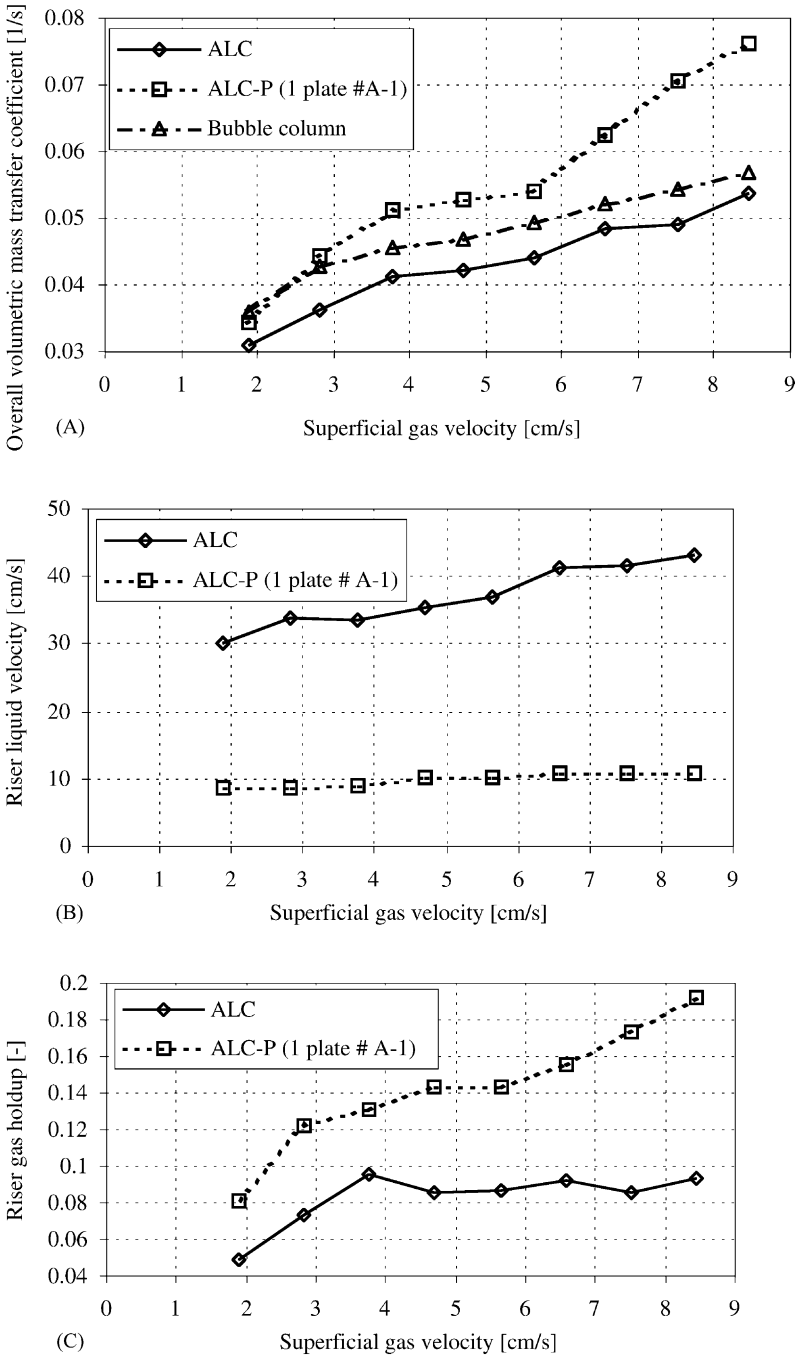

Fig. 4. Comparison between performances of ALC, ALC with a perforated plate (ALC-P), and BC.

With the results obtained from the analysis shown in Table 1, it was rather difficult to conclude on the effect of hole size in the perforated plate on each mass transfer parameter in the system. However, the overall volumetric mass transfer coefficient, $k_L a$, was often found to be the greatest with the 4 mm hole size perforated plate (Plates # B). The perforated plate with 37 holes was found to be the worst in terms of gas–liquid mass transfer. This was because this kind of plate provided the smallest increase in the mass transfer area when compared with the plates with less number of holes. It was possible that this plate contained too large free area where each hole was too close to each other, and therefore did not induce bubble breakage as much as the other configurations of plate. Nevertheless, the ALC with 13 and 21 hole perforated plates did not seem to have different mass transfer behavior.

To investigate the effect of the number of plates, the ALC was operated with one, two and three perforated plates

Table 1
Comparisons between gas and liquid mass transfer in ALC and ALC with perforated plate(s) (ALC-P)

U_{sg} (cm s^{-1})	$k_L a_c$ [a]	1 Plate				2 Plates				3 Plates			
		$k_L a$	$\%k_L a_{diff}$ [b]	$\%a_{diff}$ [c]	$\%k_{L,diff}$ [d]	$k_L a$	$\%k_L a_{diff}$ [b]	$\%a_{diff}$ [c]	$\%k_{L,diff}$ [d]	$k_L a$	$\%k_L a_{diff}$ [b]	$\%a_{diff}$ [c]	$\%k_{L,diff}$ [d]
Comparison between mass transfer parameters from conventional ALC and ALC-P + A32 with Plate # A-1													
1.889	0.031	0.034	11.392	74.746	−36.255	0.057	84.628	107.625	−11.077	0.057	83.495	89.575	−3.207
2.826	0.036	0.045	23.269	70.631	−27.757	0.058	61.404	89.312	−14.742	0.063	74.654	62.266	7.634
3.764	0.041	0.051	23.851	78.359	−30.561	0.061	47.396	82.843	−19.387	0.065	57.958	79.946	−12.219
4.702	0.042	0.053	25.296	72.064	−27.181	0.065	54.046	67.924	−8.264	0.071	66.943	69.389	−1.444
5.640	0.044	0.054	23.069	70.057	−27.631	0.066	49.099	73.475	−14.052	0.076	72.725	82.863	−5.544
6.577	0.049	0.062	28.607	75.413	−26.684	0.069	42.828	81.832	−21.451	0.084	72.575	94.713	−11.369
7.515	0.049	0.071	44.207	110.478	−31.486	0.073	50.082	108.315	−27.954	0.094	92.685	123.827	−13.913
Comparison between mass transfer parameters from conventional ALC and ALC-P with Plate # B-1													
1.889	0.031	0.057	82.848	72.583	5.948	0.057	84.898	132.695	−20.541	0.059	92.233	103.624	−5.594
2.826	0.036	0.062	70.499	46.889	16.073	0.067	86.842	95.155	−4.260	0.068	89.104	83.386	3.118
3.764	0.041	0.060	43.928	52.532	−5.640	0.077	87.308	91.437	−2.156	0.075	81.362	87.389	−3.217
4.702	0.042	0.061	43.635	45.613	−1.359	0.076	78.971	76.796	1.230	0.084	97.823	70.748	15.857
5.640	0.044	0.062	41.224	59.376	−11.390	0.084	91.125	87.268	2.060	0.089	102.578	87.989	7.761
6.577	0.049	0.070	44.477	67.562	−13.777	0.094	92.704	93.599	−0.462	0.095	95.280	100.753	−2.726
7.515	0.049	0.076	54.986	102.004	−23.276	0.094	92.072	132.558	−17.409	0.102	107.874	139.521	−13.213
8.453	0.054	0.078	44.077	109.059	−31.083	0.109	101.820	134.668	−13.998	0.105	95.414	146.257	−20.646
Comparison between mass transfer parameters from conventional ALC and ALC-P with Plate # C-1													
1.889	0.031	0.055	77.265	83.370	−3.329	0.057	85.356	94.059	−4.485	0.063	104.693	119.932	−6.929
2.826	0.036	0.058	59.488	62.251	−1.703	0.064	76.362	80.430	−2.254	0.075	108.310	90.958	9.087
3.764	0.041	0.059	42.114	62.049	−12.302	0.064	55.902	88.611	−17.342	0.077	85.131	109.398	−11.589
4.702	0.042	0.061	43.457	50.538	−4.704	0.068	60.850	67.912	−4.206	0.081	92.381	87.631	2.531
5.640	0.044	0.065	46.751	59.366	−7.916	0.074	68.730	83.523	−8.060	0.093	112.328	102.127	5.047
6.577	0.049	0.069	42.003	88.915	−24.832	0.084	72.815	85.360	−6.767	0.095	96.362	107.987	−5.589
7.515	0.049	0.080	64.385	106.878	−20.540	0.087	77.002	132.625	−23.911	0.106	116.728	152.634	−14.213
8.453	0.054	0.086	59.580	104.604	−22.005	0.089	64.501	118.439	−24.693	0.112	107.947	162.995	−20.931
Comparison between mass transfer parameters from conventional ALC and ALC-P with Plate # A-2													
1.889	0.031	0.054	76.052	51.002	16.589	0.056	82.632	82.630	0.001	0.064	106.472	103.653	1.385
2.826	0.036	0.050	39.058	67.836	−17.147	0.059	63.435	83.401	−10.886	0.070	92.521	72.829	11.394
3.764	0.041	0.054	29.576	77.019	−26.801	0.067	61.345	97.249	−18.202	0.077	86.563	82.969	1.964
4.702	0.042	0.055	29.752	56.434	−17.056	0.077	81.732	76.796	2.792	0.079	86.110	70.759	8.990
5.640	0.044	0.058	31.607	66.511	−20.962	0.087	97.289	82.278	8.235	0.086	96.047	91.877	2.173
6.577	0.049	0.060	22.699	68.691	−27.264	0.095	96.551	103.137	−3.242	0.087	80.080	95.923	−8.086
7.515	0.049	0.071	45.552	114.157	−32.035	0.097	98.270	144.203	−18.809	0.103	110.564	144.816	−13.991
8.453	0.054	0.074	37.393	106.828	−33.571	0.108	101.216	135.973	−14.729	0.104	93.390	134.294	−17.458
Comparison between mass transfer parameters from conventional ALC and ALC-P with Plate # B-2													
1.889	0.031	0.062	100.906	46.706	36.945	0.058	86.812	66.687	12.074	0.054	74.563	101.291	−13.278
2.826	0.036	0.064	77.562	46.879	20.890	0.064	77.285	64.181	7.982	0.057	57.687	74.369	−9.567
3.764	0.041	0.064	53.907	62.055	−5.028	0.066	60.256	88.571	−15.015	0.076	84.486	88.878	−2.325
4.702	0.042	0.065	54.401	43.211	7.814	0.067	59.548	69.173	−5.689	0.078	84.256	73.355	6.288
5.640	0.044	0.069	56.823	61.760	−3.053	0.075	69.809	75.961	−3.496	0.086	95.650	95.671	−0.011
6.577	0.049	0.073	50.350	64.186	−8.427	0.074	51.948	90.078	−20.060	0.103	112.541	97.128	7.819
7.515	0.049	0.075	54.015	103.229	−24.216	0.083	70.515	106.907	−17.588	0.111	126.536	146.055	−7.933
8.453	0.054	0.078	44.820	104.604	−29.220	0.088	64.036	71.429	−4.313	0.127	135.611	133.128	1.065
Comparison between mass transfer parameters from conventional ALC and ALC-P with Plate # C-2													
1.889	0.031	0.054	75.000	55.324	12.668	0.059	90.615	96.313	−2.903	0.060	94.175	80.295	7.698
2.826	0.036	0.061	68.075	41.290	18.957	0.066	83.380	55.369	18.028	0.064	76.039	75.838	0.114
3.764	0.041	0.063	53.362	56.615	−2.077	0.067	62.494	59.891	1.628	0.066	58.986	87.346	−15.138
4.702	0.042	0.063	50.181	40.808	6.657	0.066	55.387	47.646	5.243	0.073	73.687	69.422	2.517
5.640	0.044	0.066	50.310	54.619	−2.786	0.068	54.362	63.498	−5.588	0.086	95.593	80.264	8.504
6.577	0.049	0.070	44.064	67.532	−14.008	0.073	50.660	72.360	−12.590	0.091	86.727	89.839	−1.639
7.515	0.049	0.076	55.156	92.267	−19.302	0.082	67.075	112.170	−21.254	0.093	89.926	135.617	−19.392
8.453	0.054	0.085	58.234	93.505	−18.227	0.087	61.777	99.662	−18.974	0.092	71.494	124.785	−23.708
Comparison between mass transfer parameters from conventional ALC and ALC-P with Plate # A-3													
1.889	0.031	0.035	13.657	57.497	−27.836	0.040	29.126	50.771	−14.356	0.037	20.442	110.479	−42.777
2.826	0.036	0.040	10.360	66.451	−33.698	0.042	17.636	18.483	−0.715	0.046	26.537	77.312	−28.636
3.764	0.041	0.040	−2.177	59.338	−38.607	0.045	7.966	29.722	−16.771	0.047	14.457	94.632	−41.193
4.702	0.042	0.041	−2.130	42.008	−31.081	0.048	13.642	33.693	−14.998	0.049	15.570	77.149	−34.761

Table 1 (*Continued*)

U_{sg} (cm s^{-1})	$k_L a_c$[a]	1 Plate				2 Plates				3 Plates			
		$k_L a$	$\%k_L a_{diff}$[b]	$\%a_{diff}$[c]	$\%k_{L,diff}$[d]	$k_L a$	$\%k_L a_{diff}$[b]	$\%a_{diff}$[c]	$\%k_{L,diff}$[d]	$k_L a$	$\%k_L a_{diff}$[b]	$\%a_{diff}$[c]	$\%k_{L,diff}$[d]
5.640	0.044	0.044	1.045	58.194	−36.126	0.054	22.974	45.935	−15.733	0.053	21.195	92.991	−37.202
6.577	0.049	0.046	−5.565	60.812	−41.276	0.056	14.489	59.355	−28.155	0.054	11.861	95.756	−42.857
7.515	0.049	0.048	−1.962	86.198	−47.347	0.061	23.825	91.657	−35.392	0.056	15.243	132.683	−50.472
8.453	0.054	0.050	−6.907	89.057	−50.759	0.061	13.009	90.393	−40.644	0.059	10.100	129.384	−52.002
Comparison between mass transfer parameters from conventional ALC and ALC-P with Plate # B-3													
1.889	0.031	0.053	71.305	16.516	47.023	0.062	100.647	30.208	54.097	0.052	67.098	84.894	−9.625
2.826	0.036	0.054	49.307	−11.882	69.440	0.072	98.338	56.834	26.464	0.063	73.269	62.195	6.827
3.764	0.041	0.054	30.866	−7.395	41.316	0.068	63.845	69.921	−3.576	0.070	70.416	75.510	−2.902
4.702	0.042	0.055	29.516	−8.538	41.606	0.071	67.475	60.348	4.445	0.071	67.830	70.692	−1.677
5.640	0.044	0.058	30.622	17.741	10.941	0.072	64.414	68.446	−2.394	0.071	61.427	81.545	−11.082
6.577	0.049	0.058	19.882	22.569	−2.192	0.077	58.217	75.854	−10.030	0.076	57.007	95.861	−19.837
7.515	0.049	0.059	20.624	44.823	−16.710	0.084	71.843	123.678	−23.174	0.078	60.033	130.258	−30.499
8.453	0.054	0.063	17.465	40.128	−16.173	0.085	58.698	114.869	−26.142	0.085	58.234	131.884	−31.761
Comparison between mass transfer parameters from conventional ALC and ALC-P with Plate # C-3													
1.889	0.031	0.048	54.693	−18.011	88.676	0.056	79.935	30.166	38.235	0.044	42.638	56.858	−9.066
2.826	0.036	0.051	40.720	−16.083	67.689	0.058	60.803	49.443	7.602	0.058	59.903	27.447	25.466
3.764	0.041	0.055	32.317	14.360	15.703	0.064	53.604	26.644	21.288	0.065	57.172	31.251	19.750
4.702	0.042	0.056	32.395	2.263	29.464	0.065	53.159	10.646	38.422	0.065	54.815	34.156	15.400
5.640	0.044	0.065	47.206	−10.812	65.052	0.071	60.609	39.464	15.161	0.069	57.504	40.258	12.296
6.577	0.049	0.065	34.378	3.445	29.902	0.076	56.018	36.609	14.208	0.073	49.835	37.394	9.055
7.515	0.049	0.071	44.360	47.213	−1.938	0.080	63.568	90.217	−14.010	0.076	55.241	89.429	−18.048
8.453	0.054	0.075	38.322	25.628	10.104	0.092	70.674	103.075	−15.955	0.078	44.356	91.977	−24.806

[a] Overall volumetric mass transfer coefficient from the conventional ALC.
[b] The percentage difference of $k_L a$ in the ALC-P comparing to $k_L a_c$.
[c] The percentage difference of the specific interfacial area (a) in the ALC-P comparing to that obtained from the conventional ALC.
[d] The percent difference of k_L in the ALC-P comparing to k_L obtained from the conventional ALC.

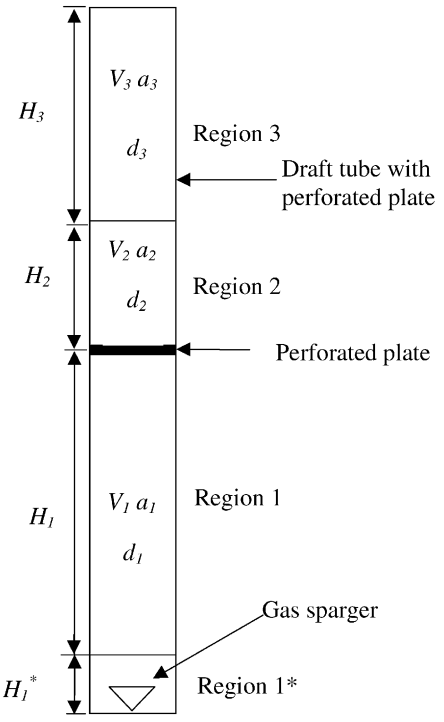

Fig. 5. Regions of bubbles of different sizes in riser of ALC with one perforated plate.

installed in the riser. The ALC with only one perforated plate was found to give the smallest rate of overall gas–liquid mass transfer while systems with two and three plates did not display different mass transfer performance. Each perforated plate had its role of breaking bubbles and increasing the number of plates resulted in a higher mass transfer area. In addition, the perforated plate blocked the flow pathway which should have induced more mixing in the system and it was then expected that the mass transfer coefficient would have been high. However, liquid circulating velocity in the ALC with perforated plate was rather small which, on the other hand, reduced the level of mixing and also the mass transfer coefficient. These two effects (more mass transfer area but small mass transfer coefficient) cancelled out each other which made it difficult to draw a clear conclusion on the overall influence of the number of plates on the mass transfer coefficient.

4. Conclusion

With the technique proposed in this work, it was possible to explain more convincingly about the effect of perforated plates on gas–liquid mass transfer in the ALC. It was shown that $k_L a$ in the system with a perforated plate could be as much as twice the value obtained from the conventional

system. The analysis showed clearly that this increase in the rate of gas–liquid mass transfer in the ALC with perforated plate was due principally to the increase in the specific interfacial area between bubbles and liquid. The mass transfer coefficient, k_L, in the system with perforated plates was found to be smaller than that obtained from the conventional system. It was also shown that there existed optimal configurations of perforated plates in terms of number of holes, hole size, and the number of plates in the ALC that provided the highest gas–liquid mass transfer rate in the ALC.

References

[1] M.E. Orazem, L.E. Erickson, Oxygen-transfer rates and efficiencies in one- and two-stage airlift towers, Biotechnol. Bioeng. 21 (1979) 69–88.
[2] Y. Bando, M. Nishimura, H. Sota, S. Suzuki, Flow characteristics of countercurrent bubble column with perforated draft tube, Chem. Eng. Sci. 47 (1992) 3371–3378.
[3] S. Goto, P.D. Gaspilo, The effect of static mixer on mass transfer in a draft tube bubble column and in external loop column, Chem. Eng. Sci. 47 (1992) 3533–3539.
[4] T.K. Ghosh, B.R. Maiti, B.C. Bhattacharyya, Gas hold-up in converging-diverging tube airlift fermenter, Biotechnol. Bioeng. 7 (1993) 301–307.
[5] T.K. Ghosh, B.R. Maiti, B.C. Bhattacharyya, Studies on mass transfer characteristics of a modified airlift fermenter, Bioproc. Eng. 9 (1993) 239–244.
[6] C.P. Chen, S.J. Yang, W.T. Wu, A novel rectangular airlift reactor with mesh baffle-plates, Biotech. Tech. 11 (1997) 439–441.
[7] H.L. Tung, S.Y. Chiou, C.C. Tu, W.T. Wu, An airlift reactor with double net draft tubes and its application in fermentation, Bioproc. Eng. 17 (1997) 1–5.
[8] H.L. Tung, C.C. Tu, Y.Y. Chang, W.T. Wu, Bubble characteristics and mass transfer in an airlift reactor with multiple net draft tubes, Bioproc. Eng. 18 (1998) 323–328.
[9] C.H. Lin, H.Y. Fang, T.F. Kuo, C.Y. Hu, Oxygen transfer an mixing in a tower cycling fermenter, Biotechnol. Bioeng. 18 (1976) 1557–1572.
[10] M. Zhao, K. Niranjan, J.F. Davidson, Mass transfer to viscous liquids in bubble columns and air-lift reactors: influence of baffles, Chem. Eng. Sci. 49 (1994) 2359–2369.
[11] G. Hebrard, D. Bastoul, M. Roustan, Influence of the gas sparger on the hydrodynamic behavior of bubble columns, Trans. IChemE 74 (1996) 406–414.
[12] T. Otake, S. Tone, K. Nakao, Y. Mitsuhashi, Coalescence and breakup of bubbles in liquids, Chem. Eng. Sci. 32 (1977) 377–383.